Experimental Determination of the Ionospheric Effects and Cycle Slip Phenomena for Galileo and GPS in the Arctic

Beeck, S. S.; Mitchell, C. N.; Jensen, A. B.O.; Stenseng, L.; Pinto Jayawardena, T.; Olesen, D. H.

Published in:
Remote Sensing

Link to article, DOI:
10.3390/rs15245685

Publication date:
2023

Document Version
Publisher's PDF, also known as Version of record

remote sensing

MDPI

Technical Note

Experimental Determination of the Ionospheric Effects and Cycle Slip Phenomena for Galileo and GPS in the Arctic

S.S. Beeck [1,*], C.N. Mitchell [2], A.B.O. Jensen [1,3], L. Stenseng [1,4], T. Pinto Jayawardena [5] and D.H. Olesen [1]

[1] Department of Space Research and Technology, Technical University of Denmark, Building 328 Elektrovej, 2800 Kongens Lyngby, Denmark
[2] Department of Electronic and Electrical Engineering, University of Bath, Bath BA1 7AY, UK
[3] AJ Geomatics, 4000 Roskilde, Denmark
[4] Peak Wind, Mikkel Bryggers Gade 4, 1460 Copenhagen, Denmark
[5] Athena Space Limited, Torquay TQ2 7TD, UK
* Correspondence: saschu@space.dtu.dk

Abstract: The ionosphere can impair the accuracy, availability and reliability of satellite-based positioning, navigation and timing. The Arctic region is particularly affected by strong ionospheric gradients and phase scintillation, posing a safety issue for critical infrastructure and operations. Ionospheric warning and impact maps can provide support to Arctic operations, but to produce such maps threshold values have to be determined. This study investigates how such thresholds can be derived from the GPS and Galileo satellite signals. Rapid changes in total electron content (TEC) or scintillation-induced receiver tracking errors could result in cycle slips or even loss of lock. Cycle slips and data outages are used as a measure of impact on the receiver in this paper. For Galileo, 73.6% of the impacts were cycle slips and 26.4% were outages, while for GPS, 29.3% of the impacts were cycle slips and 70.7% were outages. Considering the sum of cycle slips and outages, it is worth noting that the sum of impacts for Galileo signals is larger than for GPS. A range of possible explanations have been examined through hardware-in-the-loop simulations. The simulations showed that the GPS L2 signal was not adequately tracked during rapid TEC changes and TEC changes were underestimated, thus the GPS cycle slips, derived from L1 and L2 derived TEC changes, were not all registered. These results are important in designing threshold values for TEC and for scintillation impact maps as well as for the operation of GNSS equipment in the Arctic. In particular, the results show that ionospheric changes could be underestimated if GPS L1 and L2 were used in isolation from other dual frequency combinations. It is the first time this analysis has been made for Greenland and the first time that the dual frequency derivation of ionospheric delay using GPS L1 and L2 has been shown to underestimate large TEC gradients. This has important implications for informing GNSS operations that rely on GPS to provide reliable estimates of the ionosphere.

Keywords: GNSS; Galileo; scintillation; sigma phi; ionosphere; cycle slip; signal tracking; Greenland; Arctic; space weather

Citation: Beeck, S.S.; Mitchell, C.N.; Jensen, A.B.O.; Stenseng, L.; Pinto Jayawardena, T.; Olesen, D.H. Experimental Determination of the Ionospheric Effects and Cycle Slip Phenomena for Galileo and GPS in the Arctic. *Remote Sens.* **2023**, *15*, 5685. https://doi.org/10.3390/rs15245685

Academic Editor: Fabio Giannattasio

Received: 1 October 2023
Revised: 15 November 2023
Accepted: 29 November 2023
Published: 11 December 2023

1. Introduction

The Global Navigation Satellite System (GNSS) signals travel more than 20,000 km through space towards our receivers on Earth. During the first ∼95% of the journey, they travel relatively unhindered through near vacuum. However, when they reach the last ∼5%, they encounter the Earth's atmosphere. One layer of the atmosphere that has a significant impact on radio signals is the ionosphere. The GNSS signals interact with free electrons that have resulted from solar extreme ultraviolet radiation, and impact ionisation from precipitation, ionising the upper atmosphere. The amount of free electrons the signals encounter is quantified by the Total Electron Content (TEC), defined as the total number of free electrons in an imaginary cylinder with a cross-section area of one square metre

around the signal path. It is measured in TEC Units (TECU), which is 10^{16} electron per square metre.

GNSS signals travelling through the ionosphere will experience refraction as a function of the electron density along the signal path. When there are rapid fluctuations in the electron density or TEC structures with sizes around the first Fresnel radius, the signal can be subject to changes in the refractive index and diffraction. This can lead to fluctuations on the phase and amplitude of the signal [1,2]. These fluctuations of the phase and amplitude are termed scintillation. In the Arctic region phase, scintillation is the dominant type of scintillation [3], occurring primarily in the night side of the auroral oval and in the cusp [4,5].

In order to estimate phase scintillation of a received signal the fluctuations on the GNSS signal phase can be quantified using a scintillation index. The σ_ϕ index is a widely used phase scintillation index, based on the ensemble standard deviation of the detrended phase measurements. An increase in σ_ϕ indicates increased high-frequency fluctuations of the GNSS signal phase.

When GNSS signals arrive at the receiver, the effect of the phase scintillation on the positioning solution will depend on the receiver tracking architecture and the bandwidth of the carrier tracking loop [6]. This means that the effect of scintillation can differ depending on the receiver type, and this has been investigated in other studies [6–8]. However, it is widely acknowledged that phase scintillation on GNSS signals may cause cycle slips, or in the worst case result in a complete loss of lock in the receiver [3,9,10]. A cycle slip is a momentary disruption of phase tracking which does not cause loss of lock, and hence does not require re-acquisition. Several methods for detecting cycle slips exist. In the analysis in this paper, the UNAVCO approach is followed [11] where cycle slips are detected by changes in TEC above a certain threshold. In [12,13], a clear relation between σ_ϕ and cycle slips in the Canadian Arctic region was shown. Furthermore, ref. [14] found σ_ϕ to be a good indicator of loss of lock for GNSS receivers located within 20–100 km of a GNSS station tracking the scintillation activity.

Precise and reliable satellite-based positioning infrastructure is a critical capability to ensure safety in the Arctic. Ionospheric scintillation poses a threat to this infrastructure at high latitudes due to the possible degradation of GNSS reliability and positioning accuracy [3,10,12,14,15]. As a step towards local GNSS scintillation impact maps and warnings in Greenland, this study aims to statistically investigate the relations of phase scintillation with cycle slips and data outages for GPS and Galileo in Greenland. The signals chosen for this study are L1(C/A) (1575.42 MHz) and L2(P) (1227.6 MHz) for GPS and E1(OS) (1575.42 MHz) and E5a (1176.45 MHz) for Galileo, from now on referred to as L1, L2, E1 and E5a. These are chosen because they are the most widely used in the region, and there are still receivers in the Arctic that are not compatible with the newer GPS L2C and L5 signals. Previous studies have investigated the effect of scintillation on different signals; however, according to [16], the majority have been focused on the low latitudes, i.e., [17–19]. In [20], Rate of TEC index (ROTI) and ROT were investigated in the low latitude region and used to define a threshold for cycle slip event detection. While [21] relates TEC measurements to scintillation indices in the equatorial region using multiple constellations.

The novelty of this study is the analysis of the effects of phase scintillation on both GPS and Galileo frequencies related to cycle slips in signal monitoring for a full year of data from Greenland, combined with a simulation of the effects on GPS and Galileo signals. In the experimental analyses of the study, data from the Space Weather Forecasting for Arctic Defence Operations (SWADO) network has been used. The SWADO network has gathered scintillation data since the Autumn of 2021. The location of the stations in the network, which is currently being extended with more stations, can be seen in Figure 1.

Figure 1. Location of the SWADO stations along the coast of Greenland marked with stars, and the magnetic latitudes shown by dotted lines. The station used in this study is marked by a red circle.

2. Data and Methods

2.1. GNSS Stations and Data Used

The stations in the SWADO network are equipped with Septentrio PolaRx5S receivers, which are categorised as GNSS Ionospheric Scintillation and TEC Monitor (GISTM) receivers. The output files used in this study are in ionospheric scintillation monitoring record (ISMR) format and contain 1 min σ_ϕ indices computed from 100 Hz GNSS data. The indices are computed at the stations to lower the amount of data that is transmitted from Greenland. This setup of the SWADO stations was chosen with a future near real-time service in mind.

For this study, the scintillation data are obtained from one of the stations in the SWADO network, located on the west coast of Greenland in Kangerlussuaq (KLQ2). The data for cycle slip detection is obtained from one of the stations (klsq) in the Greenland GNSS Network (GNET) with a PolaRx5 receiver. The use of a non-specialised (non-scintillation) receiver (such as the PolaRx5) for cycle slip detection allows for assessment of the impact on that type of receiver; this is more relevant for applied users. The two stations are co-located, sharing a Leica LEIAR25.R4 leit antenna with the geographic coordinates (66.9956°N, −50.6202°E). The station site will be referred to by its SWADO station code, KLQ2, from now on. The KLQ2 station was chosen because it is located in an area with frequent auroral activity. This is expected to provide more scintillation impact events during the data period, improving the foundation for statistical analysis. The KLQ2 station is also located on top of a mountain structure, providing good visibility in all directions. Furthermore, the fact that the GNET and SWADO receivers share an antenna ensures that the two GNSS receivers at the KLQ2 site collect data under the exact same conditions.

The study is based on one year of GPS and Galileo data in the format of ISMR, Receiver Independent Exchange format (RINEX) and navigation files. The analyses of the study utilise twenty-seven GPS satellites: G01–09, G12–21, G23–26, G29–32; and twenty Galileo satellites: E02–05, E07–09, E11–13, E15, E21, E24–27, E30–31, E33 and E36.

The SWADO network, shown in Figure 1, is a GNSS network established in the Autumn of 2021. There had not previously been a network of GNSS receivers in Greenland sampling at a high enough frequency to compute σ_ϕ. The data period for this study starts on the 8th of November 2021 and ends one year later on the 7 November 2022. The choice of exactly one year was taken to avoid any time of the year being over- or under-represented.

This precludes any yearly variations from affecting the analysis. The phase scintillation in the night side auroral oval and cusp region have different seasonal patterns [5] and, given the location of KLQ2, the data set could contain scintillation of both regions. This is supported by the most northern ionospheric pierce point being at 83 degrees magnetic latitude and the most southern at 68 degrees magnetic latitude at an ionospheric shell height of 300 km when an elevation mask of 15 degrees is applied. However, despite the precautions to represent each season equally, there will still be an overall increase in solar activity throughout the period as a result of the 11-year solar cycle.

Signals from low-elevation satellites can be subject to non-ionospheric disturbances such as multipath. To filter out these effects, an elevation mask was utilised in the analyses. Due to the geometry of both the GPS and Galileo constellations, the satellite-tracks peak at lower elevations in the sky when observed from higher latitudes. To include as much data as possible in the analyses, it was chosen to investigate the distribution of cycle slips at the station site to find the optimal cutoff angle for this particular site. This was performed by computing a 2D histogram of cycle slips as a function of satellite elevation and azimuth angles, with North at 0 degrees azimuth increasing towards East [22]. The 2D histogram is computed based on data from the entire one-year data period. Any low-elevation obstructions of the GNSS signals at the station are assumed to be due to permanent structures like houses or antenna towers and therefore constant in time. Thus, a set elevation mask is determined from the data. The 2D cycle slip histogram is shown in Figure 2.

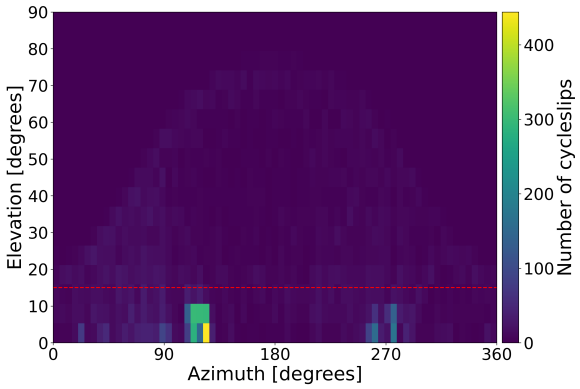

Figure 2. 2D histogram of the number of GPS and Galileo cycle slips seen from KLQ2 throughout the data period as a function of azimuth and elevation of the satellite transmitting the affected signal. The red line illustrates a 15-degree elevation mask.

Figure 2 displays a higher number of cycle slips in specific azimuth directions seen from KLQ2. The directional increases in cycle slips are attributed to permanent structures on the ground, which can be filtered out using an elevation mask of 15 degrees. This elevation cutoff angle is lower than what is used in many other studies of the ionosphere [9,10,23]. However, this is justified since the station is placed on high ground in an area with little disturbance, with the intention of being a stationary permanent GNSS station. The 15-degree elevation cutoff angle is therefore used to filter the data throughout the rest of the study.

2.2. Estimation of Phase Scintillation

The σ_ϕ index is computed as the standard deviation of the detrended carrier phase averaged over a defined time interval. The detrending is performed using a sixth-order Butterworth filter with a cutoff frequency of 0.1 Hz. The cutoff frequency can affect the σ_ϕ index [10,24], and 0.1 Hz is chosen because it is the default in the PolaRx5S and has been commonly used [5,25], which ensures the results of the study are widely applicable. The σ_ϕ index is generally computed over 60 s; however, there are several types of σ_ϕ indices in the ISMR files: Phi60, Phi30, Phi10, Phi03 and Phi01. The difference is the intervals over which σ_ϕ is computed. As an example, Phi03 is the average of the 20 standard deviations

computed over 3 s intervals during the last minute, while Phi60 is the standard deviation over the entire last minute [25]. In this study, it is chosen to consistently use Phi60 and it will henceforth be referred to as σ_ϕ.

In this study, σ_ϕ for GPS is a measure of the phase fluctuations on L1, and for Galileo it is on E1. In the first analysis, which investigates the probability of cycle slips as a function of σ_ϕ for GPS and Galileo, the mean of the σ_ϕ values is computed within 15 min intervals for each satellite. The data stream from the SWADO network provides 1 min indices inside 15 min files. The number of cycle slips and the σ_ϕ values were therefore investigated in 15 min intervals. This is consistent with the applied aims of this work, where we want to associate elevated scintillation activity with impacts on receivers with a future view to producing scintillation impact maps. The mean was chosen because it is representative of all the σ_ϕ values in the interval and more robust to outliers in the data than the maximum would be. In the second analysis, which investigates cycle slips and data outages as a function of time of day, the mean σ_ϕ is computed based on σ_ϕ from all satellites binned by the minute of day of the measurement. The mean is taken of each bin, giving 1440 mean σ_ϕ values.

2.3. Identification of Cycle Slips and Data Outages

In this study, impacts are identified through an examination of cycle slip and data outages. The cycle slips are found by the software 'Translation, Editing and Quality Checking' (TEQC) (version 2019Feb25) [11] as ionospheric delay (IOD) slips. The TEQC programme computes the IOD from the phase observation equation shown in Equation (1) [26]

$$L_f = R + c(dt_r + dt_s) - I_f + N + m_f + n_f\lambda_f \tag{1}$$

where L_f is the phase observable, R is the geometric distance between the satellite and receiver, c is the speed of light, dt_r and dt_s are the receiver and satellite clock errors, I_f is the ionospheric delay, N is the tropospheric delay, m_f is the phase multipath, and $n_f\lambda_f$ is the phase ambiguity in wavelengths. The subscript f is used to denote the frequency. Since the ionosphere is dispersive to radio frequencies the ionospheric delay is frequency-dependent. The phase delay for GNSS signals is given in Equation (2).

$$I_{L_f} = \frac{-40.3}{f^2} TEC \tag{2}$$

If it is assumed that the signals at two frequencies follow approximately the same path through the ionosphere then the TEC is the same for the two frequencies, giving the following relation, in Equation (3), between the ionospheric delays at two frequencies.

$$I_1 f_1^2 = I_2 f_2^2 \tag{3}$$

Since TEC is unknown, two frequencies are needed to determine the ionospheric delays. The phase observations at two frequencies are therefore combined in Equations (4)–(6) in order to isolate the ionospheric delay, where $\alpha = \frac{f_1^2}{f_2^2}$.

$$L_1 - L_2 = -I_1 + I_2 + m_1 - m_2 + n_1\lambda_1 - n_2\lambda_2 \tag{4}$$

$$\frac{1}{\alpha - 1} L_1 - L_2 = -I_1 + \frac{1}{\alpha - 1}(m_1 - m_2 + n_1\lambda_1 - n_2\lambda_2) \tag{5}$$

$$I_1 = \frac{1}{\alpha - 1}(L_1 - L_2 - m_1 + m_2 - n_1\lambda_1 + n_2\lambda_2) \tag{6}$$

The IOD is the time derivative of the ionospheric delay. It is assumed that the change in phase multipath is minimal over two consecutive epochs and the time derivative of the ionospheric delay on frequency 1 can therefore be expressed as in Equation (7).

$$I_{(1)}OD = \frac{1}{\alpha - 1}[(L_1 - L_2)_j - (L_1 - L_2)_{j-1}]/(t_j - t_{j-1}) \quad (7)$$

The above equations are presented as the basis of the TEQC IOD computations in [26]. The software defines an IOD slip as a change in Equation (7) that exceeds 400.0 cm/min. This is chosen to allow a certain degree of temporal variation in the ionosphere and satellite and receiver motion. The RINEX data are cut into 15 min intervals and the sum of IOD slips in each interval is found for every GPS and Galileo satellite to receiver link. The first analysis uses this cycle slip count, to statistically estimate the probability of cycle slips as a function of mean σ_ϕ.

To gain a more complete view of the potential impact of GNSS scintillation, episodes with total loss of lock, in this study referred to as outages, were also identified. This was performed by computing the satellite positions from the navigation files and comparing the satellites that should be visible above 15 degrees elevation with the satellite observations that are actually present above 15 degrees in the ISMR files. The data has a 1 min resolution of satellite outages for the full data period, which is used together with the cycle slips in the second analysis.

As with all data collected in an uncontrolled environment, data are subject to error sources, some of which are challenging to identify and mitigate. Therefore, there can be GNSS signal outages which could be caused by other sources than the ionosphere. To support the analysis, a GNSS simulator was therefore used to investigate further.

2.4. Scintillation Simulation

The data set of this study is not large enough to completely isolate the effects of the constellations and signals. Therefore, the study is enhanced with a separate third analysis using a GNSS simulator to test GPS and Galileo signals under the exact same conditions in a fully controlled environment. The simulator is a Spirent GSS7000 unit [27], which can be used to emulate the effects of the same ionospheric scenario on the tracking of GPS and Galileo satellite signals in a PolaRx5S receiver. This is the same type of receiver that is used in the SWADO network.

To simulate the ionospheric conditions, a user command define (UCD) file was created and imported into the simulator module. The file consists of 13 columns where the last two define the carrier offset and code offset for specific satellites at specific times defined in the previous columns. A description of the UCD format and use of the simulator for ionospheric research at low latitudes can be found in [28].

The relationship between ionospheric TEC and the code propagation delay of a radio signal at GPS frequencies is given by Equation (8), while the phase propagation delay was given in Equation (2).

$$I_{R_f} = \frac{40.3}{f^2} TEC \quad (8)$$

In order to simulate TEC changes in the ionosphere, and thus changes in code delay and phase advance at the receiver, the code and carrier offsets are changed in accordance with their relationship to the frequency of the signal. These numbers for code and carrier offsets are input at the signal simulation rate using the input format of the UCD file.

To create a more realistic scenario, a snip of real carrier offset, observed during a scintillation event, was superimposed on a decrease in carrier offset, which together with an increase in code offset imitated an increase in TEC. The mix of scintillation and TEC increase was selected to simulate a realistic scintillation scenario with both rapid fluctuations and plasma drift. The scintillation profile and TEC are both scaled with respect to the radio frequency. The scintillation and TEC ramping scenario is repeated three times in the UCD files with increasing amplitude, to test where the GPS and Galileo links will break.

In the GSS7000 interface, a time was chosen when GPS satellite G16 and Galileo satellite E27 were both at high elevations for the duration of the simulation. Using the orbit parameters, the GSS7000 simulated the signal from one of the satellites for each constellation while imposing the carrier and code offsets from the UCD file on the respective signal. The simulated RF signal was fed into a PolaRx5S receiver, which computed ISMR and RINEX data files. The RINEX data were used to estimate relative TEC.

3. Results

3.1. Probability of Cycle Slips as a Function of σ_ϕ

The 15 min intervals with cycle slips were binned according to the mean σ_ϕ of the interval. The probability of cycle slips for each bin was found by dividing the number of intervals containing cycle slips by the total number of intervals. The result can be seen in Figure 3.

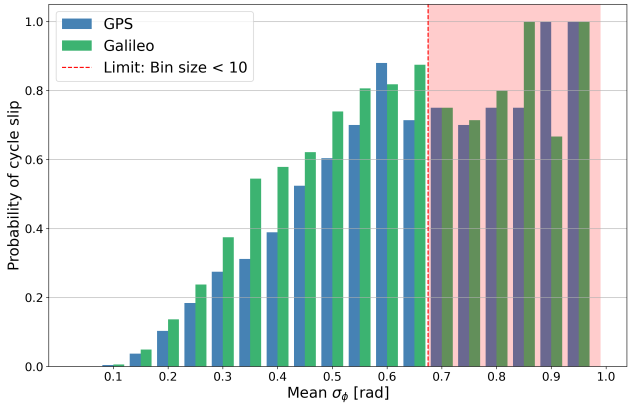

Figure 3. Probability of cycle slips as function of σ_ϕ for GPS and Galileo. The red area marks the bins containing less than ten values.

Figure 3 shows that the maximum chance of cycle slips lies for σ_ϕ from around 0.6 radians and up. For times with a mean σ_ϕ under 0.6 radians, the chance of cycle slips is seen to be consistently larger for Galileo than GPS. There can be several reasons for this which will be discussed in Section 4. The bins marked in red contain less than ten of the 15 min intervals. In some of the cases with high σ_ϕ values, the small amount of data in the bins results in a 100% probability of cycle slips. This illustrates a limitation of the data, namely that the data set does not cover a solar maximum, and therefore has a lack of very high scintillation events. The lack of events with high σ_ϕ can also be a result of losses of lock in the receiver during intense phase scintillation. Therefore, the number of outages in the data set is also investigated.

3.2. Cycle Slips and Outages in Numbers

Table 1 lists the number of cycle slips detected, the number of 15 min intervals that contain one or more cycle slips, and the number of outages for GPS and Galileo. As part of the analysis, the observation time for GPS and Galileo was also investigated. There are more GPS than Galileo satellites in the data set, but the Galileo satellites are on average visible for a slightly longer time. Overall the Galileo observation time was 77% of the total GPS observation time. This is partly due to the selection of satellites as discussed in Section 2.1. The correction was applied in the middle column of Table 1, to improve the comparability of GPS and Galileo. The correction involved multiplying the event number by the ratio of total events for Galileo divided by the total events for GPS. Hence, the middle column shows the expected number of cycle slips from GPS over a comparable observation interval to the Galileo results in column 3. The occurrence of cycle slips for GPS and Galileo shows that there are 3.6 times as many cycle slips for Galileo as for GPS when including the correction for differences in Galileo and GPS observation time. The results

therefore indicate that the Galileo satellite signals experience more cycle slips (8183) than GPS satellite signals (2197). However, the Galileo satellite cycle slips occur over a similar number of 15 min intervals (1149) as that of GPS (921) over a comparable observation time.

Table 1. Number of cycle slips, number of 15 min intervals containing cycle slips, and number of outages for GPS and Galileo. The middle column is the number for GPS corrected for the difference in observation time for GPS and Galileo seen from the station KLQ2.

	GPS	GPS Corrected	Galileo
Number of cycle slips	2862	2197	8183
Intervals with cycle slips	1200	921	1149
Number of outages	6895	5292	2929
Sum of cycle slips and outages	9757	7489	11,112

As seen in Table 1 there are around 1.2 times as many intervals that contained cycle slips for Galileo as for GPS. Galileo has 7.1 cycle slips per 15 min interval containing cycle slips, while GPS only has 2.4 cycle slips per interval containing cycle slips. Although the GPS cycle slips are fewer in number, the Galileo cycle slips are spread across a similar number of time intervals. This indicates that there are more cycle slips occurring around the same scintillation events for Galileo than for GPS. As a result, the outages for GPS and Galileo were investigated. It is seen from Table 1 that there are 1.8 times more outages for GPS than Galileo over the entire one-year data period when taking the observation time into account. This indicates distinct ratios between cycle slips and outages for the two constellations. For Galileo 73.6% of the impacts are cycle slips and 26.4% are outages, while for GPS 29.3% of the impacts are cycle slips and 70.7% are outages. Considering the sum of cycle slips and outages in Table 1, it is worth noting that the sum of impacts for Galileo signals is larger than for GPS, but the impacts on GPS are generally more severe since a higher percentage of the impacts are signal outages.

3.3. Daily Variations in Cycle Slips and Outages

In Figure 4, the number of cycle slips and outages for GPS and Galileo are shown together with the mean σ_ϕ as a function of the time of day to investigate further the relation between phase scintillation and the receiver impacts. The difference in observation time for GPS and Galileo is taken into account also in Figure 4.

Figure 4 shows daily variations in the number of cycle slips and outages for both GPS and Galileo. Referring to Figure 4a,c, the cycle slip distribution trend for GPS and Galileo is seen to be similar to each other and both are following the trend of σ_ϕ throughout the day. Both GPS and Galileo have peaks in the number of cycle slips in the afternoon around 4 pm local time and again later just before midnight, with the latter peak being higher. The peaks at certain times of day are not likely to be the result of the rise and descent of specific satellites, since the visibility of the satellites shifts every day. Referring to Figure 4b,d, there may be a relationship between phase scintillation and outages for GPS, since there is evidence of peaks at 05–09, 14–17 and 20–23 in both outages and σ_ϕ; however, looking at Galileo, the relationship between σ_ϕ and outages is not evident. This suggests that there are some outages for Galileo which are not related to phase scintillation.

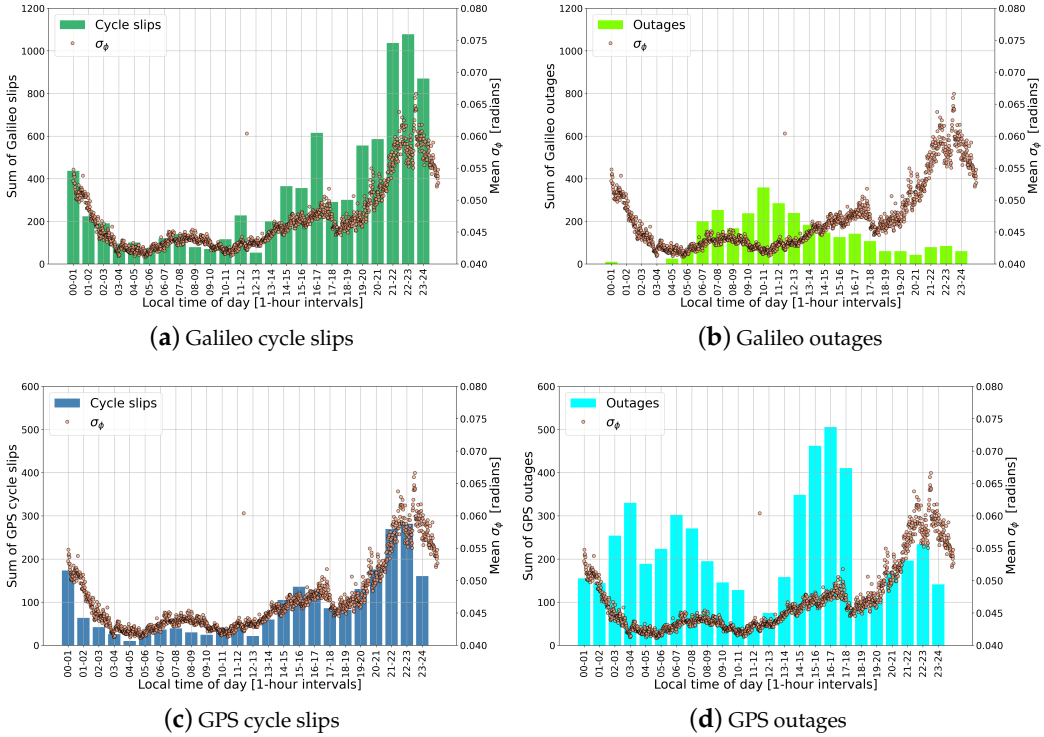

(**a**) Galileo cycle slips (**b**) Galileo outages

(**c**) GPS cycle slips (**d**) GPS outages

Figure 4. Sum of outages and cycle slips for GPS and Galileo for each hour of the day throughout the investigation period in local time (UTC-3 h). Note that the y-axis of (**c**,**d**) ranges from 0 to 600, while for (**a**,**b**) it reaches 1200. The mean σ_ϕ for each minute is overlaid, to show the relation between cycle slips, satellite outages, and phase scintillation.

3.4. Simulation of Scintillation

The results so far have indicated different responses to scintillation on GPS and Galileo signals. A controlled experiment was therefore carried out to investigate receiver response for these two signals, using a Spirent GSS7000 simulator. This allowed for identical ionospheric effects to be applied to different signals, while keeping all other signal effects benign, and to examine the receiver records. To set up this controlled test a simple ramp was applied to the TEC, with options to add in scintillation to the signals. The ramp in TEC was set to be close to the cycle slip detection levels as discussed in Section 2.3, and the receiver response to the simulated TEC ramps was investigated.

The input to the simulator is the UCD file described in Section 2.4. The time series of the TEC in the file is plotted in Figure 5a. The figure shows the constant TEC for the first two minutes and then the ramping up of TEC for two minutes, resulting in a TEC change of around 24 TECU per minute for the first two minutes. The subsequent two ramps are at 1.3 times higher gradients, so they should result in cycle slip detection.

The first TEC ramp is where the L1 and E1 signals have been subject to an increase in the code offset of 0.0013 m per 0.02 s. Corresponding higher values of code delays and phase advances resulting from the TEC ramp were applied to the L2 and E5a because these experience a larger effect due to their lower frequencies (see Equations (2) and (8)). Further, the scintillation profiles were also applied to the carrier phase offsets.

Figure 5b,c show the relative TEC computed for GPS L1 & L2 and Galileo E1 & E5a from the output RINEX files that were recorded from the simulated signals. Note that the initial value of TEC has an offset and the receiver takes time to gain lock. Nevertheless, the results show that the Galileo signals have been tracked correctly because they show the same TEC changes as were input (compare the TEC changes in Figure 5a–c). However, comparing the TEC changes in Figure 5b,c, it can be seen that the GPS signals result in an underestimation of the TEC that was simulated. Further investigation showed that the GPS receiver had a problem tracking the L2 signals through these large TEC changes and

further, that even the TEC changes alone without scintillation applied created tracking issues for L2. This may well relate to the codeless tracking requirement on L2, which is not an issue for E5a. Consequently, the cycle slip detections on GPS are not going to be triggered because the TEC changes are being underestimated, thereby showing fewer cycle slips for GPS compared with Galileo.

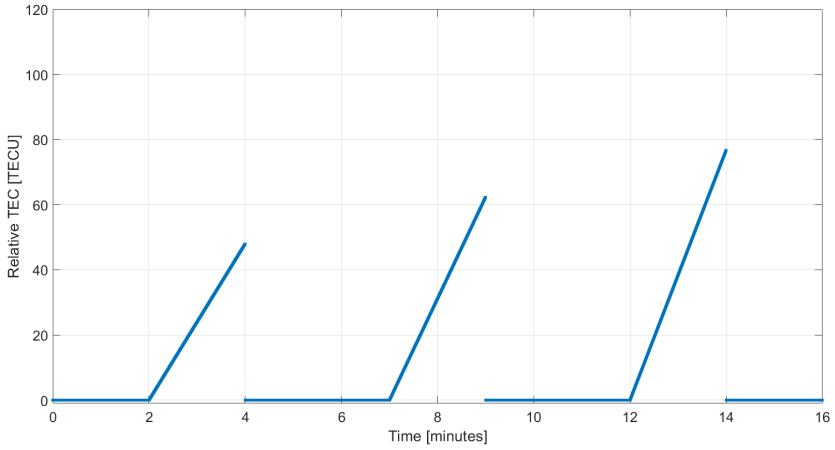

(**a**) Simulated TEC

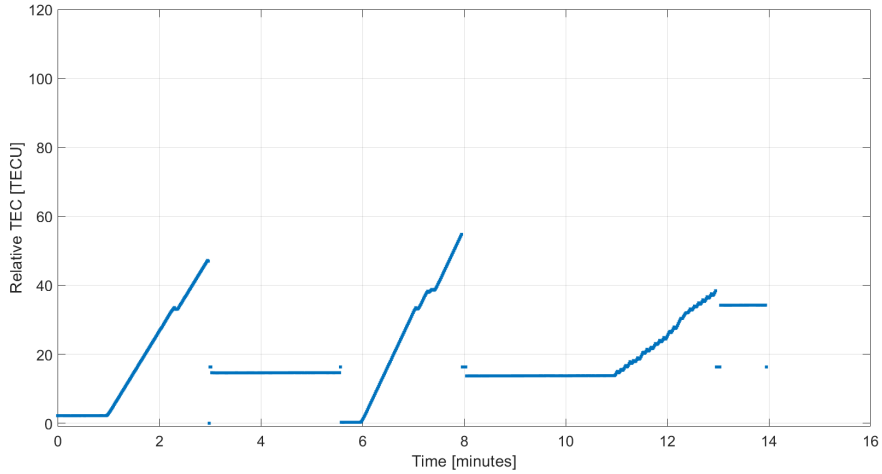

(**b**) GPS L1 & L2

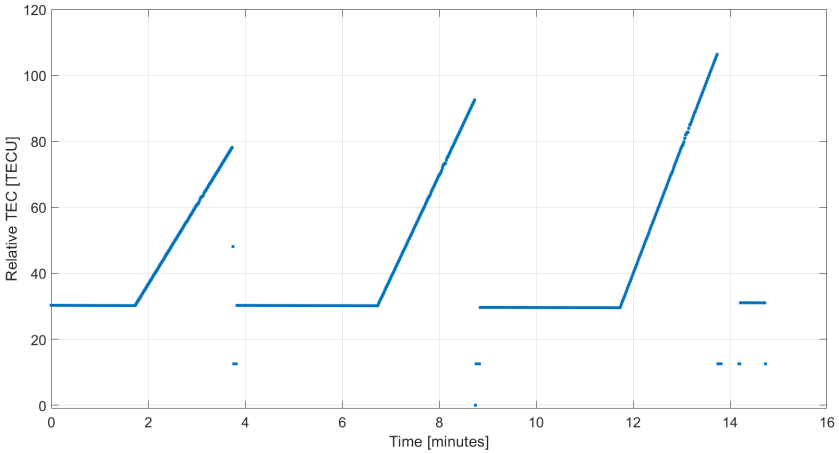

(**c**) Galileo E1 & E5a

Figure 5. Relative TEC based on L1 & L2 for GPS and E1 & E5a for Galileo.

4. Discussion

When using GNSS data for determining the impact of scintillation in the Arctic, it is a challenge that the geometry of the satellites seen from the GNSS stations is sub-optimal. Multiple GNSS constellations should therefore be considered in order to increase the amount of data. This is especially relevant in Greenland, where limited access to power and the internet restricts the possible locations of ground stations. This affects the spatial distribution of the data, resulting in spatial data gaps or regions covered mainly by low elevation data [29]. However, GNSS signals from different constellations cannot be assumed to be affected by scintillation in the same way.

This study has investigated the importance of considering the constellations used when relating σ_ϕ values to a scintillation impact level. Figure 3 showed that the probability of cycle slips increases at low scintillation levels for Galileo compared to GPS. Table 1 and Figure 4 further revealed that the tracking of signals from Galileo experiences more cycle slips, and that these cycle slips are more clustered in time than for GPS. In contrast, Table 1 showed a significantly higher number of outages of signal tracking for GPS than Galileo. These results indicate a more rapid succession of cycle slips for Galileo than for GPS. It is stated in [30] that a rapid succession of multiple cycle slips is a challenge with some cycle slip detection methods. However, the same cycle slip detection program was used for both constellations in this study, so this should not be the reason why fewer cycle slips per 15 min interval are detected for GPS compared with Galileo. It is more likely that the difference in the number of cycle slips detected for GPS and Galileo is inherent to the signal design and the tracking architecture of the receiver. This was evidenced by the results of the simulator analysis in Section 3.4.

The fact that the impact of scintillation on GNSS reliability is dependent on receiver signal tracking [31] means that preferably every receiver type used in the Arctic should be investigated to find the relationship between scintillation and its impact on receiver performance. In this study, the cycle slips were identified in data from a PolaRx5 receiver. This means that the cycle slip detection was based on data from a high-quality geodetic GNSS station, which is not necessarily representative of the receiver types applied by end users of an impact warning service. Even though the tracking architecture is not necessarily consistent between different receivers, the signal designs of the received signals are the same for all receivers capable of utilising the same frequencies.

Considering the signal designs, the Galileo E1 signal has a broader bandwidth than GPS L1, which could make E1 more vulnerable to cycle slips than L1. Furthermore, the frequency of E5a is lower than for L2, resulting in larger signal fluctuations on E5a [18,32]. Both arguments could point to the conclusion that there are more cycle slips detected for Galileo because the signals are more susceptible to cycle slips. However, it could also be a result of a higher signal strength for Galileo than for GPS, making the Galileo signal less prone to experiencing a complete loss of lock.

The simulations indicate that the increased amount of loss of lock on GPS compared to Galileo stems from L2 tracking issues. This is in line with previous studies [14,31,33]. In [14], it was concluded that, for the most severe of the high-latitude storms they examined, the tracking performance of the codeless receiver was significantly degraded, although the effect on the L1 tracking performance for both types of receivers was negligible. Likewise, it was found in a global scintillation study that the number of cycle slips on L1 was at least one level of magnitude lower than for L1–L2 [34]. A study on the effects of TEC jumps on GPS L1 and L2 in the auroral region also stated that failures in phase tracking on L2 can occur due to lower signal power or low signal-to-noise ratio on receivers for civil use since these have to utilise codeless tracking methods [35].

The GPS constellation does have alternative frequencies available today where codeless tracking techniques like cross-correlation are not needed. However, the two alternative frequencies L2C and L5 are not being transmitted from all GPS satellites yet. As of 12 April 2023, L2C is transmitted from 25 satellites and L5 from 18 satellites [36]. The complete use of these signals should be possible for L2C by 2023 and L5 by 2027 [37]. Even though

L2C and L5, once fully operational, could obviate the need for codeless or semi-codeless tracking techniques, it would require the end user segment to transition into using receivers compatible with L2C and L5. The impact of scintillation on the newer GPS signals L2C and L5 were investigated in a statistical analysis of GPS tracking during ionospheric scintillation and it was found that the L2C and L5 tracking seems to be less robust to scintillation than L1 [18].

The analyses of the study are limited to the GNSS signals utilised by the PolaRx5S and PolaRx5 receivers. The study is also limited by the selection of receiver type. Different receiver design and configuration will have an effect on the response to the ionospheric changes and the tracking response through scintillation events. The results of the study suggest that high precision GNSS users who depend on a high resilience should consider including the Galileo signals or the modern GPS signals rather than relying solely on GPS L1 and L2. The results also point to a need for weighting σ_ϕ measurements from GPS and Galileo separately if they are used in combination for evaluating the impact on the reliability of GNSS positioning. An example of this could be a future service where scintillation measurements are translated into impact maps or other types of local warning systems.

In the future, a simulator, like the one used in this study, can be useful in testing the response of different receiver types when imposing various ionospheric disturbance scenarios. To test a receiver thoroughly without a simulator, the receiver should be deployed in the region of interest, preferably for one or more solar cycles. With a simulator, a thorough testing of receivers and new signals types can be performed in significantly less time. Furthermore, the test is carried out in a controlled environment where the receiver is not left unprotected. In [7], a simulator was also used in order to test the impact of simulated scintillation on different receivers.

Further investigation into the relationship between cycle slips and the ionospheric plasma irregularities is an intriguing topic. It is well established that ionospheric plasma can cause rapid TEC changes that can result in phase jitter, and that irregularities can also cause diffractive effects that cause phase jitter and amplitude scintillation. The ionospheric state causing a scintillation event can be partly inferred using GPS observations but other instrumentation needs to be used to gather additional information about the underlying physical mechanisms. Interesting work by authors such as [38–41] have made significant advances in this topic. In future, it would be interesting to advance the understanding of cycle slip events by relating it to a model of the ionospheric irregularity structure together with a forward model of refractive and diffractive processes.

In the development towards an operational local warning system for Greenland, the next step would be to discuss the tolerance for false positives versus missing warnings with the user segment, and also to include more signals in the analysis. With time, it will only become more relevant to include the new GPS signals L2C and L5 in this type of analysis and perhaps other GNSS constellations to gain a better data coverage over Greenland.

5. Conclusions

Analyses pointing to differences in the impact of ionospheric scintillation on GPS and Galileo signals were presented in this paper. The impact was evaluated using cycle slips in a PolaRx5 receiver from GNET and outages in a PolaRx5S receiver from SWADO, both located in Kangerlussuaq (66.9956°N, −50.6202°E). For Galileo, a high percentage of the impacts were cycle slips as opposed to signal outages. This is in contrast to GPS behaviour, where the opposite is true. The Galileo phase tracking experienced a significantly larger number of cycle slips than for GPS, while GPS overall experienced more outages than Galileo did. Collectively, Galileo experienced the highest number of scintillation impacts as a result of the large number of cycle slips. Several possible explanations were investigated, and the results point towards the reason being issues in tracking the L2 signal, leading to fewer cycle slips being detected for GPS. Inconsistencies between ROTI based on L2 and

L2C were found in [42] and further discussed in [43], which provides supporting evidence for the results found in this paper. The conclusion of this study is therefore that there is a different response to ionospheric disturbances for GPS and Galileo due to the GPS signals underestimating the TEC during large TEC changes, as a result of the codeless tracking requirement on L2, which is not an issue for Galileo E5a.

Author Contributions: Conceptualisation, S.S.B., A.B.O.J. and L.S.; methodology, All authors; software, S.S.B. and C.N.M.; validation, S.S.B.; formal analysis, All authors; investigation, All authors; resources, All authors; writing—original draft preparation, S.S.B.; writing—review and editing, All authors; visualisation, S.S.B.; supervision, L.S., A.B.O.J., D.H.O., C.N.M. All authors have read and agreed to the published version of the manuscript.

Funding: C.N.M. has received funding from NERC grant number NE/W003074/1.

Data Availability Statement: The GNET dataset from SDFI which was analysed in this study is publicly available and can be found here: https://dataforsyningen.dk/data/4804, accessed on 8 November 2022. The SWADO data presented in this study are available on request from the corresponding author.

Acknowledgments: C.N.M. acknowledges support from a Royal Society Industry Fellowship. S.S.B. acknowledges DALO for funding part of her PhD studies. This study was made possible by access to data from the SWADO network which is operated by DTU on behalf of the Danish Defence and from the GNET owned by SDFI. Also important was access to the Spirent GSS7000 simulator at the University of Bath which made it possible to test the response of the GPS and Galileo signals to the same ionospheric disturbance under the exact same environment conditions. UNAVCO is acknowledged for developing and making the TEQC software version 2019Feb25 available.

Conflicts of Interest: A.B.O. Jensen was employed by the AJ Geomatics, L. Stenseng was employed by the AJ Geomatics and T. Pinto Jayawardena was employed by the Athena Space Limited. The remaining authors declare that the research was conducted in the absence of any commercial or financial relationships that could be construed as a potential conflict of interest.

Abbreviations

The following abbreviations are used in this manuscript:

GISTM	GNSS Ionospheric Scintillation and TEC Monitor
GLONASS	Global Navigation Satellite System
GNET	Greenland GPS Network
GNSS	Global Navigation Satellite System
GPS	Global Positioning System
IOD	Ionospheric Delay
ISMR	Ionospheric Scintillation Monitoring Record
RF	Radio Frequency
RINEX	Receiver Independent Exchange format
SWADO	Space Weather Forecasting for Arctic Defence Operations
TEC	Total Electron Content
TECU	TEC Units
TEQC	Translating, Editing and Quality Checking
UCD	User Command Define
UTC	Universal Time Coordinated

References

1. Titheridge, J.E. The diffraction of satellite signals by isolated ionospheric irregularities. *J. Atmos. Terr. Phys.* **1971**, *33*, 47–69. [CrossRef]
2. Kintner, P.M.; Ledvina, B.M.; de Paula, E.R. GPS and ionospheric scintillations. *Space Weather* **2007**, *5*, S09003. [CrossRef]
3. Jiao, Y.; Morton, Y.; Taylor, S.; Pelgrum, W. Characterization of high-latitude ionospheric scintillation of GPS signals. *Radio Sci.* **2013**, *48*, 698–708. [CrossRef]
4. Aarons, J. Global positioning system phase fluctuations at auroral latitudes. *J. Geophys. Res.* **1997**, *102*, 17219–17231. [CrossRef]
5. Prikryl, P.; Jayachandran, P.T.; Mushini, S.C.; Chadwick, R. Climatology of GPS phase scintillation and HF radar backscatter for the high-latitude ionosphere under solar minimum conditions. *Ann. Geophys.* **2011**, *29*, 377–392. [CrossRef]

6. Humphreys, T.E.; Psiaki, M.L.; Kintner, P.M. GPS Carrier Tracking Loop Performance in the presence of Ionospheric Scintillation. In Proceeding of the 18th International Technical Meeting of the Satellite Division of the Institute of Navigation, ION GNSS 2005, Long Beach, CA, USA, 13–16 September 2005.
7. Hinks, J.C.; Humphreys, T.E.; O'Hanlon, B.; Psiaki, M.L.; Kintner, P.M. Evaluating GPS receiver robustness to ionospheric scintillation. In Proceeding of the 21st International Technical Meeting of the Satellite Division of the Institute of Navigation, Ion GNSS 2008, Savannah, GA, USA, 16–19 September 2018; Volume 3, pp. 1390–1401.
8. Taylor, S.; Morton, Y.; Marcus, R.; Bourne, H.; Pelgrum, W.; Van Dierendonck, A.J. Ionosphere Scintillation Receivers Performance Based on High Latitude Experiments. In Proceeding of the ION 2013 Pacific PNT Meeting, Honolulu, HI, USA, 23–25 April 2013.
9. Pi, X.; Mannucci, A.J.; Lindqwister, U.J.; Ho, C.M. Monitoring of global ionospheric irregularities using the worldwide GPS network. *Geophys. Res. Lett.* **1997**, *24*, 2283–2286. [CrossRef]
10. Veettil, S.V.; Aquino, M.; Spogli, L. A statistical approach to estimate Global Navigation Satellite Systems (GNSS) receiver signal tracking performance in the presence of ionospheric scintillation. *J. Space Weather Space Clim.* **2018**, *8*, A51. [CrossRef]
11. Estey, L.; Wier, S. *Teqc Tutorial: Basic of Teqc Use and Teqc Products*; UNAVCO: Boulder, CO, USA, 2014.
12. Prikryl, P.; Jayachandran, P.T.; Mushini, S.C.; Pokhotelov, D.; MacDougall, J.W.; Donovan, E.; Spanswick, E.; St.-Maurice, J.-P. GPS, TEC, scintillation and cycle slips observed at high latitudes during solar minimum. *Ann. Geophys.* **2010**, *28*, 1307–1316. [CrossRef]
13. Prikryl, P.; Jayachandran, P.T.; Mushini, S.C.; Richardson, I.G. High-latitude GPS phase scintillation and cycle slips during high-speed solar wind streams and interplanetary coronal mass ejections: A superposed epoch analysis. *Earth Planets Space* **2014**, *66*, 62. [CrossRef]
14. Meggs, R.W.; Mitchell, C.N. GPS scintillation over the European Arctic during the November 2004 storms. *GPS Solut.* **2008**, *12*, 281–287. [CrossRef]
15. Datta-Barua, S.; Doherty, P.H.; Delay, S.H.; Dehel, T.; Klobuchar, J.A. Ionospheric Scintillation Effects on Single and Dual frequency GPS Positioning. In Proceedings of the 16th International Technical Meeting of the Satellite Division of the Institute of Navigation ION GPS/GNSS 2003, Portland, OR, USA, 9–12 September 2003; pp. 336–346.
16. Romero, R.; Linty, N.; Cristodaro, C.; Dovis, F.; Alfonsi, L. On the Use and Performance of new Galileo Signals for Ionospheric Scintillation Monitoring. In Proceeding of the Institute of Navigation Technical International Meeting (ITM 2017), Monterey, CA, USA, 30 January–2 February 2017.
17. Carrano, C.S.; Groves, K.M.; McNeil, W.J.; Doherty, P.H. Scintillation Characteristics Across the GPS Frequency Band. In Proceedings of the 25th International Technical Meeting of the Satellite Division of the Institute of Navigation (ION GNSS 2012), Nashville, TN, USA, 17–21 September 2012; pp. 1972–1989.
18. Delay, S.H.; Carrano, C.; Groves, K. A Statistical Analysis of GPS L1, L2 and L5 Tracking Performance During Ionospheric Scintillation. In Proceeding of the 2015 ION Pacific PNT Conference, Honolulu, HI, USA, 20–23 April 2015.
19. Hlubek, N.; Berdermann, J.; Wilken, V.; Gewies, S.; Jakowski, N.; Wassaie, M.; Damtie, B. Scintillation of the GPS, GLONASS, and Galileo signals at equatorial latitude. *J. Space Weather Space Clim.* **2014**, *4*, A22. [CrossRef]
20. Sinha, S.; Bhardwaj, S.C.; Vidyarthi, A.; Jassal, B.S. Ionospheric Scintillation analysis using ROT and ROTI for Slip Cycle Detection. In Proceedings of the 4th International Conference on Information Systems and Computer Networks (ISCON), Mathura, India, 21–22 November 2019.
21. Vankadara, R.K.; Jamjareegulgarn, P.; Seemala, G.K.; Siddiqui, M.I.H.; Panda, S.K. Trailing Equatorial Plasma Bubble Occurrences at a Low-Latitude Location through Multi-GNSS Slant TEC Depletions during the Strong Geomagnetic Storms in the Ascending Phase of the 25th Solar Cycle. *Remote Sens.* **2023**, *15*, 4944. [CrossRef]
22. Septentrio. *PolaRx5S Reference Guide*; Septentrio: Leuven, Belgium, 2020.
23. Yang, Z.; Morton, Y. Time lags in Ionospheric Scintillation Response to Geomagnetic Storms; Alaska Observations. In Proceedings of the 33rd International Technical Meeting of the Satellite Division of the Institute of Navigation (ION GNSS+ 2020), Online, 21–25 September 2020; pp. 3494–3501.
24. Forte, B.; Radicella, S.M. Problems in data treatment for ionospheric scintillation measurements. *Radio Sci.* **2002**, *37*, 6. [CrossRef]
25. Septentrio. *PolaRx5S User Manual*; Version 2.3; Septentrio: Leuven, Belgium, 2021.
26. Estey, L.H.; Meertens, C.M. TEQC: The Multi-Purpose Toolkit for GPS/GLONASS Data. *GPS Solut.* **1999**, *3*, 42–49. [CrossRef]
27. Spirent.com. Spirents Official Website. Available online: https://www.spirent.com/products/gnss-simulator-gss7000 (accessed on 29 August 2023).
28. Mohd Ali, A. GNSS in Aviation: Ionospheric Threats at Low Latitudes. Ph.D. Thesis, University of Bath, Bath, UK, 2018.
29. Beeck, S.S.; Jensen, A.B.O. ROTI maps of Greenland using kriging. *J. Geod. Sci.* **2021**, *11*, 83–94. [CrossRef]
30. Breitsch, B.; Morton, Y.J. Triple-Frequency GNSS Cycle Slip Detection Performance in Presence of Diffractive Ionosphere Scintillation. In Proceedings of the ION Position, Location and Navigation Symposium (PLANS), Portland, ON, USA, 20–23 April 2020.
31. Skone, S.; Knudsen, K.; de Jong, M. Limitations in GPS Receiver Tracking Performance Under Ionospheric Scintillation conditions. *Phys. Chem. Earth (A)* **2001**, *26*, 613–621. [CrossRef]
32. Hong, J.; Chung, J.; Kim, Y.H.; Park, J.; Kwon, H.; Kim, J.; Choi, J.; Kwak, Y. Characteristics of Ionospheric Irregularities Using GNSS Scintillation Indices Measured at Jang Bogo Station, Antarctica (74.62°S, 164.22°E). *Space Weather* **2020**, *18*, e2020SW002536. [CrossRef]

33. Nichols, J.; Hansen, A.; Walter, T.; Enge, P. High-Latitude Measurements of Ionospheric Scintillation Using the NSTB. *Navig. J. Inst. Navig.* **2000**, *47*, 2. [CrossRef]
34. Afraimovich, E.L.; Lesyuta, O.S.; Ushakov, I.I.; Voeykov, S.V. Geomagnetic storms and the occurrence of phase slips in the reception of GPS signals. *Ann. Geophys.* **2002**, *45*, 55–72. [CrossRef]
35. Chernyshov, A.A.; Miloch, W.J.; Jin, Y.; Zakharov, V.I. Relationship between TEC jumps and auroral substorms in the high-latitude ionosphere. *Sci. Rep.* **2020**, *10*, 6363. [CrossRef]
36. GPS.gov. Official U.S. Government Information about the Global Positioning System (GPS) and Related Topics. Available online: https://www.gps.gov/systems/gps/modernization/civilsignals/ (accessed on 6 July 2023).
37. Esper, M.; Chao, E.L.; Wolf, C.F. *Federal Radio Navigation Plan*; United States Department of Defense, Department of Transportation, Department of Homeland Security: Washington, DC, USA, 2019.
38. Deshpande, K.B.; Bust, G.S.; Clauer, C.R.; Rino, C.L.; Carrano, C.S. Satellite-beacon Ionospheric-scintillation Global Model of the upper Atmosphere (SIGMA) I: High-latitude sensitivity study of the model parameters. *J. Geophys. Res. Space Phys.* **2014**, *119*, 4026–4043. [CrossRef]
39. Deshpande, K.B.; Bust, G.S.; Clauer, C.R.; Scales, W.A.; Frissell, N.A.; Ruohoniemi, J.M.; Spogli, L.; Mitchell, C.; Weatherwax, A.T. Satellite-beacon Ionospheric-scintillation Global Model of the upper Atmosphere (SIGMA) II: Inverse modeling with high-latitude observations to deduce irregularity physics. *J. Geophys. Res. Space Phys.* **2016**, *121*, 9188–9203. [CrossRef]
40. Deshpande, K.B.; Zettergren, M.D. Satellite-Beacon Ionospheric-Scintillation Global Model of the upper Atmosphere (SIGMA) III: Scintillation simulation using a physics-based plasma model. *Geophys. Res. Lett.* **2019**, *46*, 4564–4572. [CrossRef]
41. Zernov, N.N.; Driuk, A.V. Coherence properties of high-frequency wave field propagating through inhomogeneous ionosphere with anisotropic random irregularities of electron density: 1. Theoretical background. *J. Atmos. Sol.-Terr. Phys.* **2020**, *205*, 105313. [CrossRef]
42. Yang, Z.; Liu, Z. Investigating the inconsistency of ionospheric ROTI indices derived from GPS modernized L2C and legacy L2 P(Y) signals at low-latitude regions. *GPS Solut.* **2017**, *21*, 783–796. [CrossRef]
43. McCaffrey, A.M.; Jayachandran, P.T.; Langley, R.B.; Sleewaegen, J.-M. On the accuracy of the GPS L2 observable for ionospheric monitoring. *GPS Solut.* **2018**, *22*, 23. [CrossRef]